EVOLUTION OF BUSBAR DESIGN FOR ALUMINIUM REDUCTION CELLS

Anthony R. Kjar[(1)], Jeffrey T. Keniry[(2)], Dagoberto S. Severo[(3)]

1. Gibson Crest Pty Ltd, 23 Laurel Grove, Blackburn Victoria 3130 Australia
arkjar@bigpond.com.au tel: +61 3 9878 1843
2. Alumination Consulting Pty Ltd, 2 Governors Drive, Mt Macedon, Victoria 3441 Australia
jkeniry@netcon.net.au tel: + 61 3 5426 4124
3. PCE Engenharia S/C Ltda, Rua Felix da Cunha, 322 Porto Alegre RS – Brazil
dagoberto@pce.com.br tel: +55 51 3346 1287

The application of mathematical modeling, together with practical designs and efficient fabrication methods, has had considerable impact on the improvement in capital costs of aluminum reduction cells over the last thirty years. This is particularly the case for the cell busbar design, which represents 10-15% of the total potline cost. This paper outlines the evolution of the busbar design for modern, high amperage cells. The design principles for electrical balance and optimum magnetic field distribution are discussed, by which the all-important magneto-hydrodynamic (MHD) stability of the cell is achieved. A case study based on modeling of a generic 240 kA reduction cell in several busbar configurations is presented, to illustrate these design principles.

Effective busbar designs must also take account of the many practical needs, including optimization of the busbar mass (current density), ease of fabrication, inclusion of an efficient cell bypass system, and safe electrical isolation. These needs are discussed from the perspective of the broadly similar approaches taken by the various high amperage cell designs that are in operation throughout the world.

DUTY REQUIREMENTS OF A BUSBAR SYSTEM

The busbar system provides the electrical connection from the upstream reduction cell cathodes to the downstream cell anodes. The following criteria must be met by the design:

Optimum MHD Behaviour

Intense magnetic fields (B) are generated by current carried in the busbars. These fields interact with the current density vectors (J) flowing in the molten metal pool within the cell, to generate electromagnetic volume (Laplace) forces (F=JxB). These forces define the MHD behaviour of the cell and are largely responsible for performance differences in current efficiency, cell stability and energy consumption that tend to characterize different cell technologies.

The important MHD criteria are:

Metal flow – must be adequate to promote circulation and dissolution of alumina, but not so high as to promote localized instabilities or erosion of the cell linings. Flow patterns which are symmetric about the central axes are preferred for stability, and are generally achieved by having low and anti-symmetric distribution of the By and Bz fields about these axes. "Dead spots' at the alumina feeder locations are to be avoided.

Metal topography – should be as flat as possible, to optimize the anode performance and bath circulation. This is best achieved by reducing the current density in the anode riser busbars (increasing the number of risers, and distributing them along the sides of the cell in a side-by-side cell layout).

Metal-bath interface stability – must be robust to routine cell operations such as anode change and tapping. In particular, the magnetic field within the cell should promote damping rather than propagation of any waves that may form on the interface. This is best achieved by having low values of Bz (and low Bz gradients) currents in the metal pool.

Electrical Balance via a Practical Means of Connection

The busbar design must also provide for uniform distribution of current away from the cathode collector bars, and into the anode rods at the downstream cell. Achieving this objective requires conductor paths of equal electrical resistance ($R=\rho L/A$), even though the path lengths from / to individual electrodes will be different.

In practice, uniform distribution of current into the anode rods is relatively easy to achieve. This is because the anodes are all in a parallel electrical connection and the resistance of the cell electrolyte dominates the total circuit resistance.

This is not the case for the cathodes however. Even though they are also in parallel connection, the metal pool has negligible resistance and the current distributed to each cathode will depend on the resistance of the collector bar assembly and the cathode busbar feeding the downstream cell. The design challenge is to avoid generation of horizontal currents (Jx, Jy) in the metal pool, as these contribute to MHD instability. Meeting this challenge requires:

- Equal distribution of current into each of the cathode blocks (collector bars) and …
- Equal distribution of current to each end (upstream & downstream) of each collector bar.

These criteria are achieved by providing equi-resistive busbar paths, where the degrees of freedom are the cross-sectional area of the various busbars, the path length, and (rarely) the

resistivity of the busbar material itself[*]. The cross-sectional area of the aluminium busbar is also constrained by resistive heating, which may limit the safe working temperature to around 200^0C and the current density to a maximum of around 100A/cm^2.

An Efficient Means of Isolation

As all cells in the potline are in series connection, shutdown of any cell for cathode relining requires that it be isolated from the circuit via an efficient means of electrical bypass. The current by-pass is an integral part of the busbar design, and has tended to become more complex as cells have increased in size / current, and particularly by the implementation of side risers as opposed to simple end riser configurations.

Safety in Operation

Modern potlines are operating at DC currents to 350 kiloamperes and voltages to 1500 volts, and they have considerable stored energy. As operators and machinery are frequently in contact with the busbars, their isolation from potential earths is of paramount importance to achieve a safe working environment.

Minimum Capital Cost

Typically a bus bar system for a modern smelter is made of aluminium, weighs 15,000t and costs $50m. As such it represents 10-15% of the potline cost. With increasing amperage the bus bar complexity must also increase in order to avoid high magnetic field gradients. Economic busbar design is inevitably a compromise between the mass of busbar required in order to achieve optimum electrical and magnetic field balances, against the minimum required to achieve acceptable cell performance.

The conceptual design (as developed via modeling) will consider the interaction of key cost drivers and their impact on cell performance, such as:

- The optimum number of anode risers
- Routing of the upstream cathode current either around or under the cell
- The spacing between the cells
- The average and maximum busbar current density consistent with the busbar rating and the required electrical balances in the network.

The detailed design will further consider fabrication issues, weld design etc in order to optimise the capital cost. In addition, the voltage drop within the bus bar system must be considered as a trade-off between the initial capital cost and an on-going operating cost. Sound design and integrity of electrical joints is particularly important.

[*] Different collector bar designs or connections could also be used as a means to achieve uniformity of cathode current, but are yet to be actively pursued to the authors' knowledge.

Reasonable and Economic Operation of the Cell

The bus bar system must not interfere with the normal cell operations of anode setting and tapping. The cell stability also impacts on the liquid metal inventory necessary to operate the cell efficiently, which may vary by ±50% according to the quality of the busbar design.

HISTORY OF DEVELOPMENTS

The history of developments is outlined within the context of the response to the duty requirements outlined previously. This response has enabled the amperage of cells to be increased substantially, together with improvement in performance efficiencies and MHD parameters, as shown in Table 1.

Optimum MHD Behaviour

In the last 25 years many different theories and approaches have been used to develop models in order to study MHD behaviour in reduction cells. These models have advanced to the extent that they now underpin the design of new cells with considerable reliability. The principles of MHD design have been well covered in prior publications, such as Huglen[1], Segatz[2], Potocnik[3] and La Camera[4].

Due to computational restrictions, the early models were concerned mainly with the steady state flow pattern, the metal velocity and the heave of the metal pool. MHD stability was typically predicted via empirical indices that considered the main parameters known to influence it – for example, the average value of Bz over the cell, the current, the metal height and the bath density. Such indices were not renowned for their reliability however.

The steady state models still play an essential role in cell design. Modern 3-D modelling packages (typically ANSYS) permit calculation of the magnetic fields, current distribution and force fields based on the detailed geometry of the busbars and other cell components, including field attenuation by the steel potshell, the influence of neighbouring cells and potlines, crossover busbars etc. Such models are then coupled with computational fluid dynamics packages such as Fluent or CFX to predict the steady-state MHD properties of the cell with considerable accuracy. The magnetic field may be calculated by derivative[5] or integral[6] methods. Due to different behaviour of the current through the bath and metal layers, the force field for each fluid may generate different flow patterns, whereas in older designs with higher metal velocities the bath flow is simply dragged by the metal flow. Some commercial codes for fluid mechanics simulation deal with this kind of problem in diverse ways, such as moving grids or free surface multiphase modelling, with homogeneous or non-homogeneous fluid treatment[7].

Table 1. Typical Present Performance from Different Cell Technologies

When Installed	1965-1980	1970-1985	1980-today	1990-today
Cell Layout	End to end	Side to side	Side to side	Side to side
Riser Layout	End, or End & side	End (2 or 4)	Side (2 or 4)	Side (4, 5 or 6)
Current Range kA	120-180	150-180	180-220	250-350
Cell Technologies	Alusuisse Alcan Hydro VAW VAMI	Kaiser P69 Reynolds P19 Sumitomo Nippon Mitsui	AP18/21 Alcoa 697 Comalco-Dubal CD20 VAW CA180 Reynolds P20 Kaiser P80	AP30/35 Alcoa A817 Rusal VAMI C255/C280 GAMI GP320 SAMI SY300 Hydro HAL250
Magnetic Compensation - neighbour row	Mostly yes	No	Mostly no	Mostly yes
Typical Current Density A/cm^2	0.70-0.80	0.80-0.88	0.80-0.85	0.72 (Chinese) 0.80 (Russian) 0.85 (Western)
Current Efficiency	88-93	91-94	93-95	94-96
Volts per Pot	4.5-4.7	4.4-4.6	4.2-4.3	4.1-4.3
Energy consumption DCkWh/kg	15.0	14.5	13.5	13.2
Typical Magnetic Field (G, max)				
Bx	100 - 150	100 - 150	150 - 200	180 - 220
By	100 - 200	80 - 120	20 - 40	30 - 50
Bz	80 - 120	120 - 180	15 - 30	15 - 40
Metal Velocity (cm/s average / max)	10 / 25	10 / 25	5 / 15	6 / 20
Typical Metal Heave Δh (cm max)				
Short axis / Long axis	2 / 5	2 / 8	4 / 2	4 / 2

The busbar design capability is not complete however without the support of a reliable MHD stability prediction. With modern computational power, very complex stability models are now possible, accounting for the influences of all the cell bus bar system, neighboring lines, shell shielding, anode consumption and interface deformation. Two main families of models are most commonly used. The first uses 'shallow water' theory to analyse wave propagation at the bath-metal interface[8,9], and calculates wave growth rates (doubling times) for the most unstable waveforms to compare different designs. The second approach is to develop full 3-D models that treat in detail the geometry and generally treat the background flow with a multiphase three-dimensional model[10,11]. In these models an artificial perturbation is induced on the metal surface, and the damping response monitored via fluctuation in the anode currents (ACD).

Whereas the Pechiney AP30 technology[12] has dominated greenfield smelter developments for more than a decade, there are now at least five commercial technologies operating in the +300 kA current range. The Russian and Chinese technologies are being used in national projects, and the latter are also being actively marketed for external application. Each of these technologies has different busbar configurations, and all designs are underpinned by MHD modelling.

The modern approach in design of the magnetic fields is to:

- Precisely account for the attenuation of the magnetic field by the shell and cradles. Model predictions are validated against in-situ measurement of the magnetic field within the cavity of operating cells.

- Compensate for the Bz field component of neighbouring rows, so as to achieve symmetric flow fields within the cell.

- Achieve low values of Bz (typically targeting maximum values of ± 15 Gauss) and balanced values (of equal and opposite sign) within each quadrant of the cell. This ensures that rotational force fields within each quadrant will be opposing.

- Avoid high Bz gradients in the central part of the cell, which might be generated by the location and proximity of under-cell busbars or riser flexibles for example.

- Study the effect of specific anode changes on cell stability, and optimise the magnetic field distribution accordingly.

These objectives are achieved by the discretionary spatial location of busbars (x, y and z coordinates) and the current flow within them, within the constraints imposed by economics and the need to achieve current balance. Some aspects to consider for side-to-side cells are that

- The impact of magnetic fields is reduced when the busbars are located further from the metal pool – for example, considering the effect of horizontal conductors (riser flexes, anode bridge, under-cell cathode busbars) on Bz.

- Bz fields can be reduced and balanced by current flowing in parallel busbars rather than a single bar, so that the Bz effect of passing current around the end of the cell for example can be reduced if some current is passed inboard of the end and below the shell.

- Directional current flows in the cathode busbars between cells (eg considering the downstream cathode bus of the upstream cell in proximity with the upstream cathode bus of the downstream cell) may be used to balance fields.

- By fields will be minimised by placing the busbars at the elevation of the metal pool.

Electrical Balance via a Practical Means of Connection

The evolution of the potline layout, and the resulting busbar connections, has been driven by the trend to bigger and bigger cells together with the imperative of improved working conditions. This evolution has been underpinned by the development of key technologies for alumina feeding, pot-tending cranes and, in particular, computer models that first focused the busbar design on the electrical balance, then steady-state MHD, and more recently on dynamic MHD stability[13]. Typical busbar layouts are shown in Figures 1 and 2.

Table 2. Evolution of Busbar Design

Increasing cell size & current ⟶

Period	Pre-1920	Pre-1970	1970-1985	1980-
Cell Layout	Small cells Side to side End risers	End to end End risers	Side to side End risers	Large cells Side to side Side risers
Drivers	Busbar economy (Cathode collector bus at end of cell)	Access for heavier manual operations	Hooding of cells	MHD stability
Enabling Technologies		Feeding from vehicles	Centre break & feed Alumina distribution by crane	Computer modeling Pneumatic conveying of alumina

Figure 1. Evolution of Busbar Designs

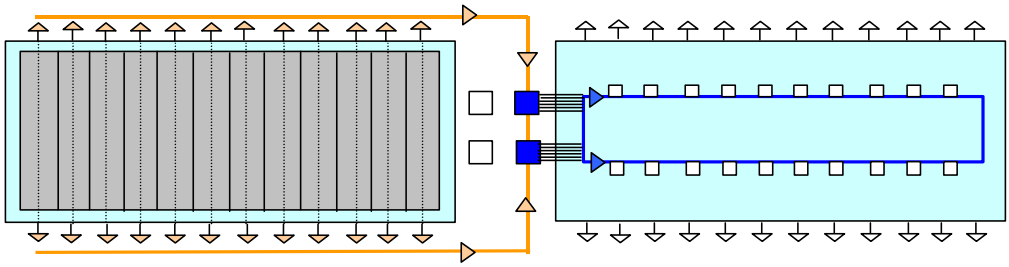

(a) Simple busbar layout for end-to end cells

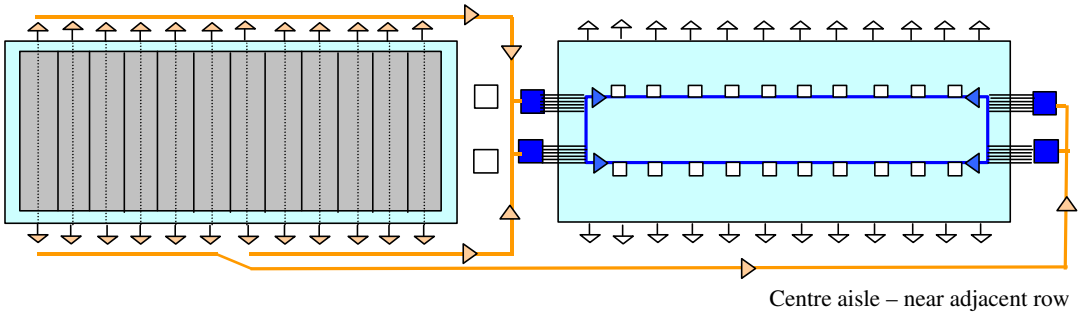

(b) End-to end cells with asymmetric busbars compensating neighbour row

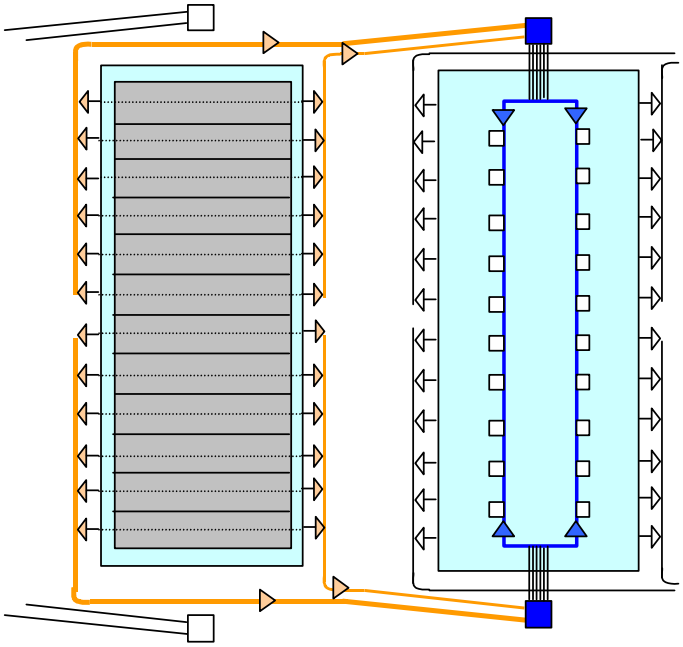

(c) Simple busbar layout for side-to-side cells with end risers

Figure 2. Evolution of Busbar Designs (continued)

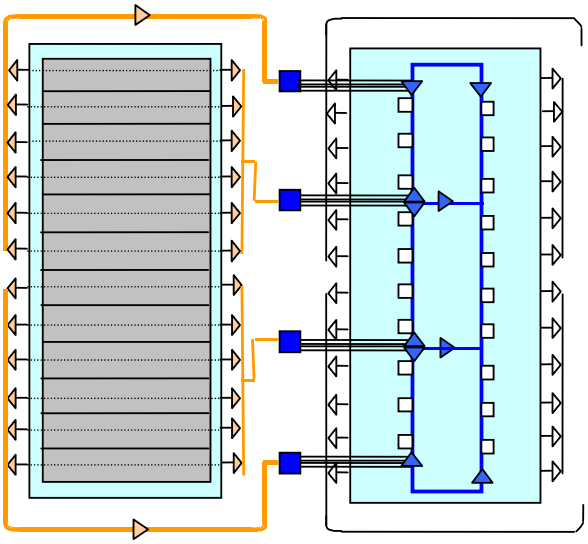

(d) Simple busbar layout for side-to-side cells with side risers. Symmetric busbar, current to ~ 250 kA.

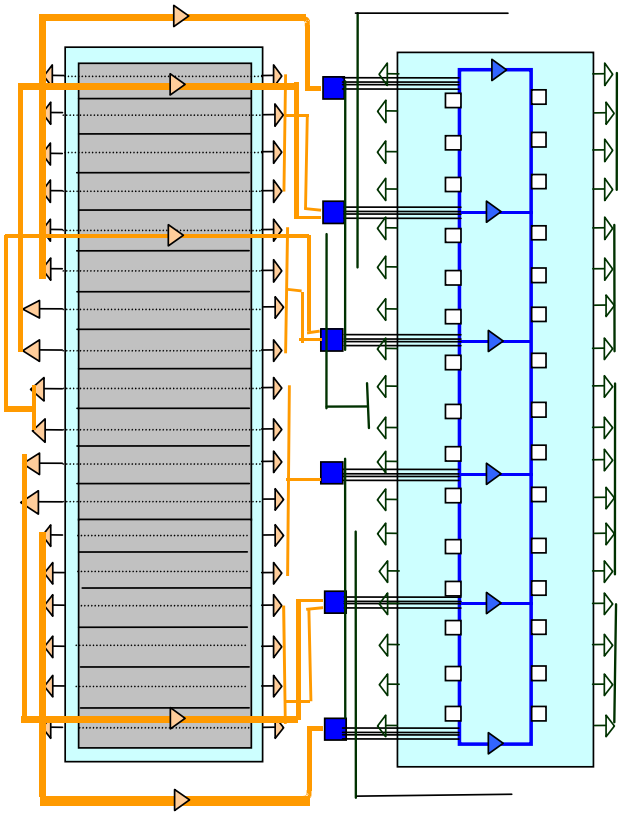

(e) Busbar layout for side-to-side cells above 300 kA. Asymmetric busbar, with some current passing under the shell and providing Bz compensation for neighbour row.

The basic design has evolved whereby cathode collector bars are connected to side risers and the anode bus. Within this basic configuration some options include

a. *Equi-resistive paths created between individual cathode bars and anode jacks on a few anodes*, using busbars of differing cross-section. This approach was taken when the first computer models focused on the importance of electrical balance, and sometimes extended to individual control of each anode height. This approach has proven to be expensive and provides little value to cell performance however, as the main resistance within the circuit from the anode riser to the bath is reasonably high and circuits are readily equalized without the need for elaborate anode feeder bus.

b. Connection of groups of cathode bars to common busbars, with the upstream cathode busbar passing around the cell, and the risers connecting to a common anode bus. The cathode bars are sized by length and / or cross-section in order to give the required electrical resistance and current flow. This design is typical of end riser cells and side-riser cells to 200 kA.

c. As above, but with some upstream cathode busbar passing under the cell to minimise the required path length. This approach has developed as cells have become larger, to minimise both the distance as well as the additional resistance that needs to be built into the downstream path to achieve a reasonable current balance. The spatial location of these under cell bus bars can be used to balance Bz fields and, if placed asymmetrically, to balance the Bz contribution from the neighbour row.

In addition there are important variants between the various technologies for:

- The number, location and shape of the anode risers
- The elevation of the cathode busbars with respect to the shell
- The design of the collector bars (single, twin and/or split; square, rectangular or round cross-section; cast iron, glue or rammed paste sealing etc)
- The connection of the steel cathode bars to the busbar flexibles (bolted copper tabs, permanent transition joints with welded collector bar connections, flash-welding of aluminium flex to the collector bars etc)
- The busbar sections (cast or machined, straight or tapered, single or multiple leaf)
- The busbar connections (bended, bolted joints, stacked plate welds, narrow gap welds, chemical welds etc)
- The degree of symmetry in the busbar layout and / or current flow in the cathode busbars

An efficient electrical balance will achieve cathode currents with a coefficient of variation of less than 10%[*] for individual values, and an upstream-downstream current split within the range 48-52%.

[*] COV=(Standard deviation*100)/Mean

An Efficient Means of Isolation

The isolation system will need to satisfy a number of design criteria:

- *Preferably, to bypass the cell without the need to take the potline off load*. This has become more important as potlines have increased in current and size, as the production loss from frequent switching of cells in or out of circuit can be substantial. The time to implement rectifier tap changes in bringing the potline back to normal current also increases as the operating current becomes higher. The impact of temporary shedding of a large quantum of power into the supply grid, or the time required to manage temporary power curtailment from a captive power plant, may also be issues depending on the smelter location.

- *The bypass operation must be safe, not labour intensive, and able to be deployed rapidly.* The bypass will involve the making of temporary joints across busbars, typically by driving bridging wedges between existing busbars or by making bolted or clamped connections to them. The connection points must have safe access and be amenable to monitoring to ensure that electrical resistance and temperature remain within acceptable limits. Depending on the design, making or breaking of the bypass can take from 5-15 minutes. If the bypass operation requires the potline to be taken off-load, the downtime must be minimized to avoid disruption to the heat balance and stability of other cells.

- *The bypass design must be cost-effective*. In the bypass mode, some existing busbars may be called upon to carry more than their normal current while others become redundant. In some cases, additional bars are fitted (either permanently or temporarily) to carry part of the bypass current. The design will need to consider the maximum current density that can safely be applied to busbars and connection joints, while economizing on the mass of busbar employed.

- *The bypass design must preserve the MHD stability of neighbour cells*. The bypass design will involve a redistribution of current in the busbars and will generally impact upon the current balance of both the upstream and downstream cells. This can have a negative effect on the operation of these cells.

A typical redistribution of busbar current when a cell is in bypass mode is indicated in the modeling Case Study, Figure A3.

Safety in Operation

Accordingly, the immediate working floor around the cells is isolated from earth, and any connections between live cell components and earth, such as fume ducts and supports for busbars and potshells, are provided with electrical insulation. Pot tending cranes have several levels of isolation between the mounting rails (earthed) and the hooks, tooling and operator cabin that may be in contact with live cells and busbars.

Wall claddings are also typically insulated at lower levels near the working floor. The potroom building frame is at earth potential however, and may be as near as 3 metres from live busbars. Damage to structural concrete leading to exposure of metal reinforcing is a particular hazard. The basement floor is also at earth potential, and typically within arms reach of live busbars. Specific and strict operating procedures are therefore required to support design safeguards.

Some of the procedures that will be in place in modern potrooms to enhance electrical safety include:

- Earthing of the potline at the end crossover, to effectively halve the total voltage drop. Continuous monitoring to detect any shift in the 'null point' location will help identify any transient earths that may appear. Such earths must be found and removed.

- Use of temporary earth straps at locations where specific maintenance work is required in proximity to potential earths. Ideally, the temporary earth unit will be fitted with its own alarm system should another earth appear on the potline while the work is in progress.

- Automatic trip of the potline current if an open-circuit condition is detected, normally in response to abnormally low current. If a fault arises on the potline resulting in an open circuit, a large amount of energy is dissipated at the point of the fault. This can lead to extensive damage to pots and endanger the life of personnel.

- Strict controls on access to potlines by maintenance contractors, and prohibiting the use of any conductive tools that may bridge distances between live surfaces and earth. Examples include aluminium ladders and electrical tools, which must be supplied via isolating transformers.

- Restricted access to the potline basement area

- Use of footwear offering high electrical resistance.

- Maintenance priority on issues that may create earths, such as cleaning of molten metal spillages from floors, prevention of rainwater access, use of rapid setting resins for floor repairs etc

Minimal Capital Cost

Prior to the establishment of the spatial configuration it is important to note that

- More risers generally involve more complexity.
- There are space limitations on the downstream side as cell spacing is reduced, particularly for wrap around busbars.

Besides choosing a spatial configuration there are a number of other features that can impact on capital cost. These include

- Minimising the mass of busbar required, through choice of high current density as aluminium, or choice of more conductive materials such as copper.
- Detailed design of the bus bar to minimise use of expensive expansion joints.
- Detailed design of the system to minimise number and type of welds for benefits in both capital cost and operating cost (by lowering the busbar resistance).
- More risers generally involve more complexity.
- There are space limitations on the downstream side as cell spacing is reduced, particularly for wrap around busbars.
- Structural design of the basement, shell supports and bus bar supports to be compatible with the required spatial configuration and any likely upgrades, to avoid designs that might trap any overflow of bath or metal into the basement, and to avoid any configuration that might comprise safety.

Bus bars are constructed from solid heavy aluminium sections. These are usually horizontally cast. Flexible joints between the bus bar, the cathodes and the cell anode beam are usually made from rolled aluminium coil. Usually the joints are welded.

Welding issues include

- Welding heavy sections is not simple. Challenges include controlling the weld pool, distortion and cracking. Techniques for new bus bar systems include electro-slag

welding as practiced in Russia and joining with a series of small (stack) plates using MIG argon shield welding which is the preferred method elsewhere.

- Each method is expensive. Typically a large stack plate weld requires 8 to 10 hours to complete as each stack plate is cut and ground to size and the previous weld is also ground to achieve the required fit-up for the next plate. In addition the stack plate system only achieves a 50 to 60% electrical connection to the parent metal. This results in electrical joint loss.

One approach to reduce the impact is to redesign the busbar to minimize the number of welds required and to minimize the number of site welds required. Another approach is to develop a new weld system. One such method, called narrow gap welding, has been pioneered by the CSIRO Division of Manufacturing together with the CRC for Welding Structures in Australia for both carbon steel and aluminium, and has application in both potshells and aluminium bus bar systems. Narrow gap welding uses a computer controlled MIG argon shield welding head to control and optimize the formation of the weld pool.

The technique has been proven in both shop and field environments in work sponsored by Comalco for the construction of new cells at Boyne Smelters Ltd[14]. With the development of advanced heads and a four axis automated guidance system, the technique is now in commercial use[15,16]. Using this technique it is possible to weld with an 18mm gap, with controlled shrinkage and minimal weld distortion when joining full size busbar sections. The manhours required is cut by 300%, due to reduced weld preparation requirements compared to the conventional approach, and a 100% rather than 50-60% electrical joint connection is achieved.

Welding also has additional challenges when joining in-situ busbar within an electrical field, as the presence of the electrical field influences the weld metal pool, making it difficult to achieve a satisfactory weld. Stopping the electrical current for an extended period is not an economic option and methods of welding insitu have to be used. Some techniques that have been tried include:

- Use of bolted connections
- Use of a Faraday cage to shield the weld pool
- Shutting the potline for a short period to complete an initial weld and then use special techniques to complete the total weld
- Use of a CAD weld system[17]

Reasonable and Economic Operation of the Cell

Compatibility with Operations.

The introduction of side risers has forced the change to multiple hoods rather than using an automatic side opening system. While this requires a little more effort it has had a beneficial environment impact on dust and fluorine emissions.

More recently the move to double anode changing, using either two separate anodes or two anodes on the one rod and a specialised 'Pacman' cleaning device has narrowed the selection of anode riser - anode combinations.

Suitable combinations in commercial cells operating at 280-320 kA include

32 anodes, 4 risers	X X ® X X X X ® X X X X ® X X X X ® X X
36 anodes, 4 risers	X X ® X X X X ® X X X X X X ® X X X X ® X X
36 anodes, 4 risers	® X X X X X X ® X X X X X X ® X X X X X X ®
40 anodes, 5 risers	X X ® X X X X ® X X X X ® X X X X ® X X X X® X X
48 anodes, 6 risers	X X ® X X X X ® X X X X ® X X X X ® X X X X ® X X X X ®XX

Choice of aluminium busbar materials

Considerable cost savings can also be gained by optimizing the busbar manufacture, consistent with the service needs. Improved dimensional control and shape of the bus bar will reduce subsequent welding requirements and joint losses.

The typical materials used include:

Horizontal cast busbars - generally made of 99.5% or 99.7% alloy to 1350 A/Al 99.5 EC or 1370 A/Al 99.7 EC.

Anode beams and rods are generally made of 99.8% alloy to 1370 A/Al 98, or a 6000 series alloy if greater strength is required.

The electrical conductivity of busbar products can vary by as much as 10% (range 31-35 $m/\Omega mm^2$) for alloys of similar specification[18]. The alloy properties also need to be chosen so as to minimise creep in operation. The normal design is 80°C, while above 150-200°C creep becomes a significant problem.

The Optimum Current Density

The current density will vary in different busbar sections as dictated by the requirement to achieve current balance. Typically, it will vary from a minimum of around $20A/cm^2$ (in the upstream cathode bus) to a maximum of around $80A/cm^2$ in the downstream cathode bus directly feeding the risers of the next cell, with a volume-weighted average of around $30A/cm^2$. In older plants where capacity creep has been achieved, these values may be higher but the risk of overheating busbar will constrain what can safely be achieved. The increase in electrical resistance of busbar as the temperature increases must also be considered.

The optimum weighted-average current density (and the design value for feeder and cross-over busbars) becomes an economic trade-off between investment cost and operating cost. For example, targeting a higher average current density will lower the required mass of busbar but will increase the power consumption due to resistive heating of the busbars. For a typical modern potline, about 5% of the total power consumption is lost as ohmic heating

of the aluminium busbars. If the potline is producing 250,000 tonnes of aluminium at 13.5 ACMWh/t and $20/MWh, the annual cost of the busbar power loss will be around $3.5 million. Given that there is designer discretion of around ± 20% in the average volume-weighted current density, there is significant leverage in finding the optimum economic design.

Output from a simple financial model to determine the optimum current density is shown in Figure 3. It is based on a typical modern potline using 2000 metres of busbar and operating at a current of 320 kA, with the following inputs:

- Busbar installed cost $US 3500 per tonne
- Power cost $US 20/MWh
- 25 year life and discount rate of 10% for calculation of net present cost

With these assumptions, an optimum busbar current density of around 40A/cm^2 is indicated.

Figure 3. Economic Busbar Current Density

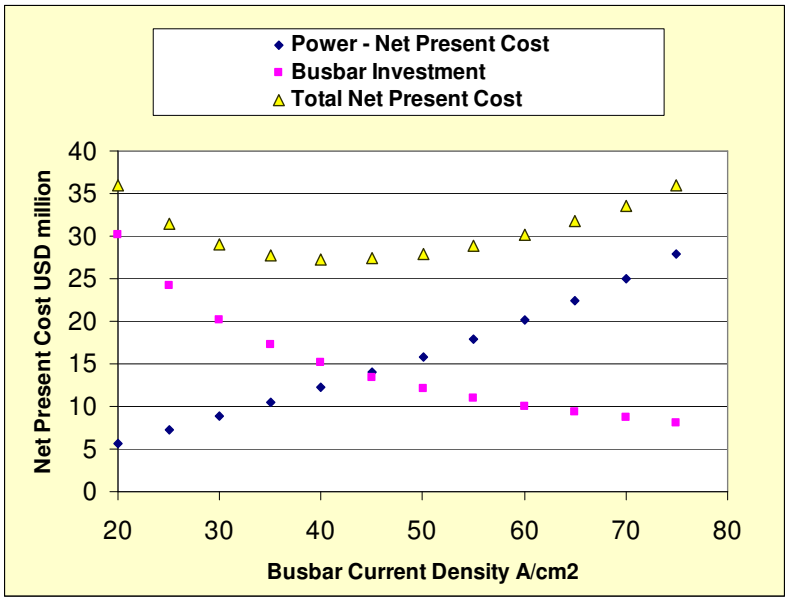

MODIFICATIONS TO EXISTING PLANTS

A number of plants have reported changes to the busbar system with beneficial results. Some of these changes have been made off-line, while others have been made on-line. Generally the costs of shut down of a potline (or progressively, sections of cells) to make busbar modifications outweigh the benefits of improved performance, so the preference is to find viable improvements that can be carried out while the pot remains in operation, or when it is bypassed during routine relining. In both cases, the types of work that can be

done are constrained by the difficulties in welding in the magnetic field, as previously noted.

Some examples of successful busbar improvements made on an operating potline include

- Fitting additional busbar leaves to address current density constraints caused by capacity creep. This will usually occur in the downstream cathode busbar, and care must be taken to avoid introducing electrical imbalance in the cathode currents.

- Relocation of under-cell busbars (or fitting of new bars) to provide Bz compensation of the neighbouring row of cells[19].

- On side-to-side cells with end risers, re-routing some or all of the upstream collector bus under the cell and outwards along the central axis to avoid high Bz fields at the upstream corners of the cell[20].

- Conversion of side-to-side cells from end riser to side riser configuration[21]

- Fitting additional risers to end-to-end cells[22]

There are still many opportunities to increase current in existing potlines by improving the busbar performance. A typical pathway forward is

  - MHD assessment and modeling of existing cell design to identify issues
  - modelling of improvement options
  - trials on at least five cells to verify performance
  - detailed fabrication and construction plan considering safety issues, interfaces with operations, and welding techniques in the magnetic field
  - installation.

CASE STUDY – BUSBAR OPTIONS FOR A 240 kA SIDE-TO-SIDE CELL

This case study compares MHD simulations for three busbar options for a hypothetical 240kA cell:

(i) End risers
(ii) Four side risers, with all upstream cathode busbar passing around the cell ends
(iii) Four side risers, with some upstream cathode busbar passing under the cell

Figure A1. Schematic Busbar Layouts

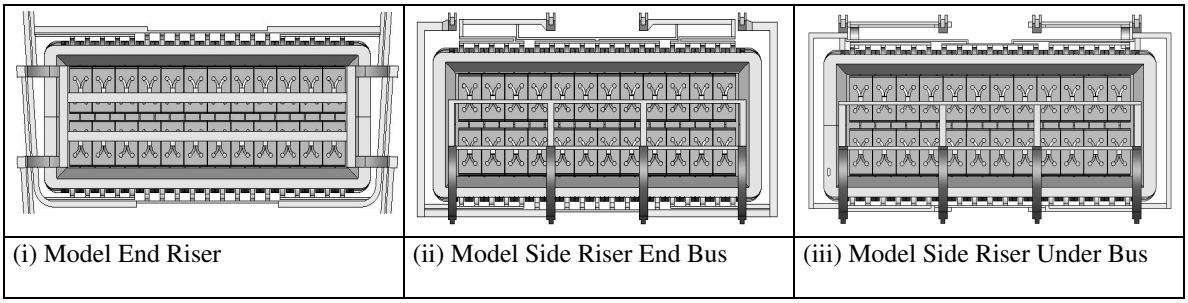

(i) Model End Riser	(ii) Model Side Riser End Bus	(iii) Model Side Riser Under Bus

The 3-D models were developed by coupling the commercial codes ANSYS and CFX. The electric-magnetic models were built in ANSYS. Steady state and transient MHD flows were calculated with CFX. Metal and bath were treated as multiphase flow using the homogeneous VOF (Volume of Fluid) model to calculate the bath-metal interface. The studies of cell stability were done using CFX in transient regime.

Figure A2. Model Structures

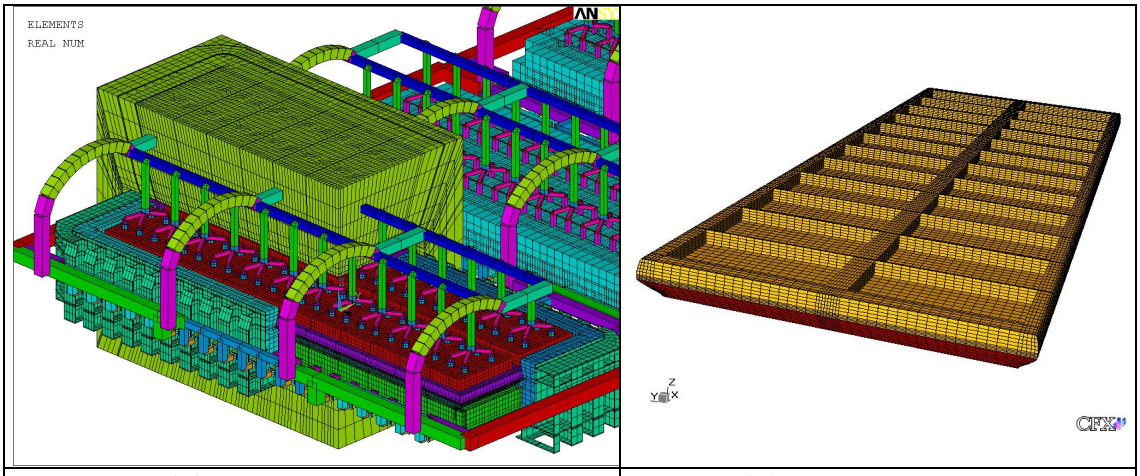

ANSYS model	CFX model

Model Assumptions. Each cell is assumed to operate at 240kA, and a metal level of 200mm. An ACD of 45mm was assumed for the Side Riser options, whereas a higher ACD was necessary to obtain stability model convergence for the End Riser option. Each cell uses the same shell, same anodes and same pot-to-pot spacing of 6.2m. The return line was considered to be at 60m, resulting in a Bz imbalance of around 8G. For the Side Riser Under Bus option, this Bz imbalance was compensated by using asymmetric current. Two pots either side of the target cell were included in the models. The maximum current density used was 75 A/cm^2 for all bars except for anodic busbars and risers where 60 A/cm^2 was used due to some bypass situations.

Current Density in Busbars

The current density in the busbar network is shown in Figure A2, while a comparison for the 'End Busbar' option in operating and bypass mode is shown in Figure A3.

Figure A2. Busbar Current Density

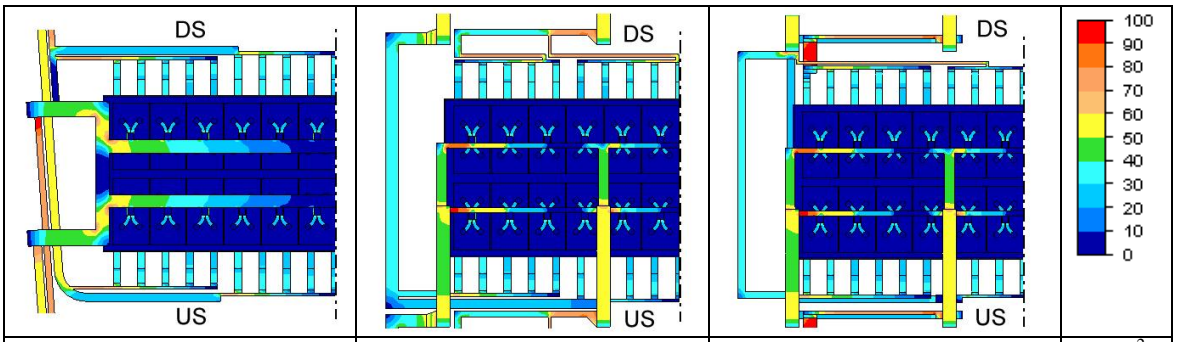

End Riser Half-model	Side Riser End Bus Half-model	Side Riser Under Bus Half-model	(A/cm^2)

Figure A3. Busbar Current Density in Bypass Mode – End Busbar Option

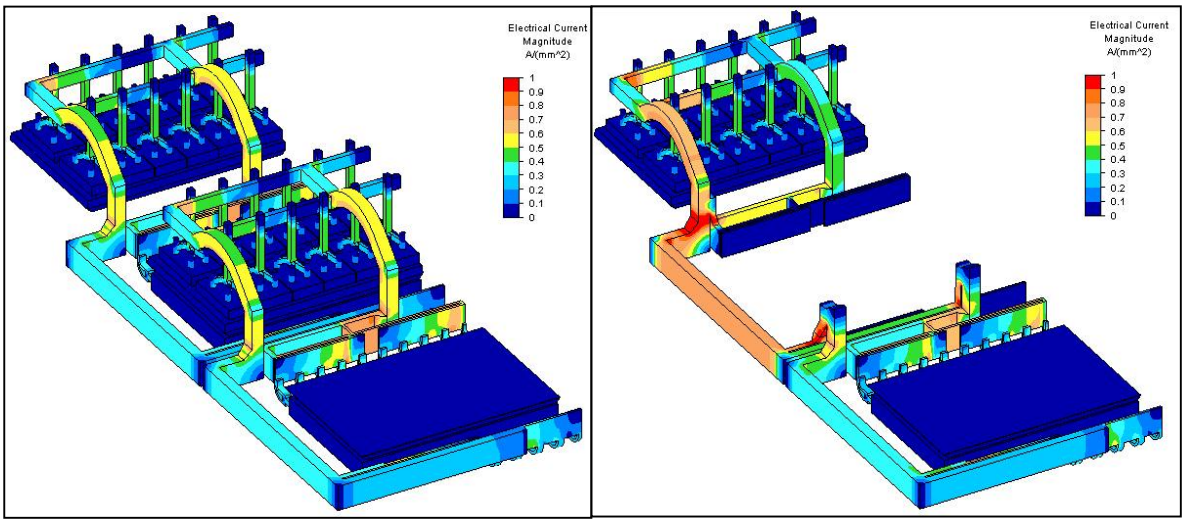

Distribution of Currents in Collector Bars & Anode Rods

Model	Collector Bars Std dev	Anode Rods Std dev	US current	DS current	Average current density (A/cm^2)	Maximum current density (A/cm^2)
End Riser	2.05 %	0.45 %	49.7 %	50.3 %	33.2	75.0
Side Riser End Bus	2.97 %	0.53 %	49.2 %	50.8 %	41.2	75.0
Side Riser Under Bus	2.44 %	0.57 %	49.8 %	50.2 %	39.6	75.0

Magnetic Fields

A comparison of the magnetic fields is shown in Figure A4. Major changes are apparent when the risers are relocated from the ends to the sides of the cell:

- Stronger Bx field along the sides of the cell
- Major reduction in By field, a driver of metal velocity and heave over the long axis of the cell
- Major reduction in Bz field at the upstream corners, a driver of MHD instability.

Comparing the two side-riser options, there are subtle but important differences in the Bz fields. For the option using undercell busbar, there is

- A reduction in Bz intensity at the upstream corners
- A more antisymmetric field distribution.

Figure A4 Magnetic Fields - Bx By Bz contour maps

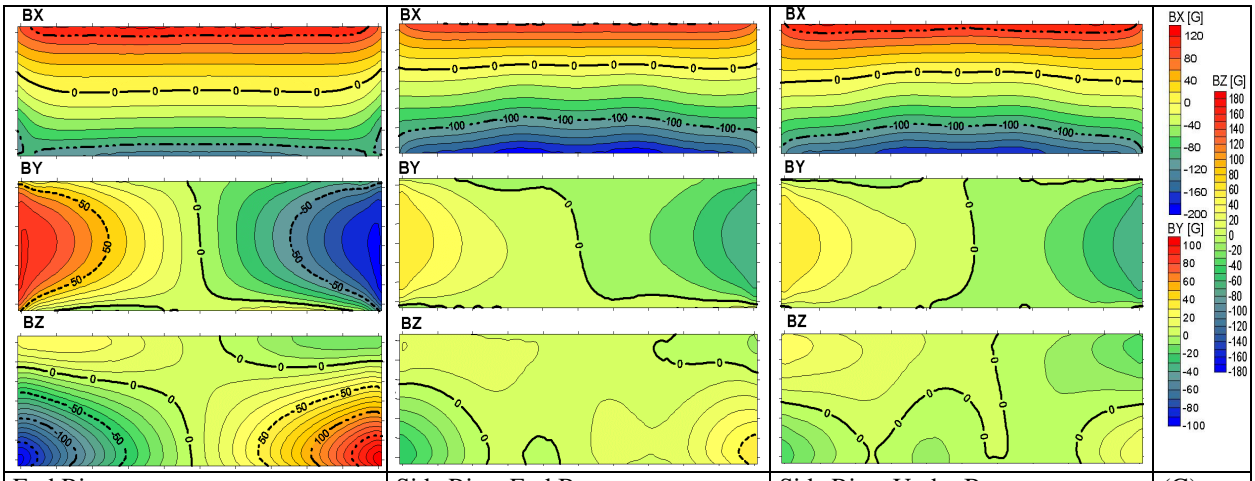

End Riser	Side Riser End Bus	Side Riser Under Bus	(G)
Bx max = -131.2 G By max = - 92.1 G Bz max = +185.8 G	Bx max = -195.0 G By max = -39.8 G Bz max = +56.7 G	Bx max = -177.6 G By max = -39.4 G Bz max = +36.0 G	

Metal Circulation

Metal flow is reduced in the side riser options as a result of reduction in the strong force fields associated with current concentration in the end riser design, Figure A5. For the Under Bus option, the flow is further improved and is also made more symmetric by the Bz compensation of the neighbour line.

Figure A5. Metal Flow

End Riser Vmax = 0.267 m/s Vaverage= 0.108 m/s	DS 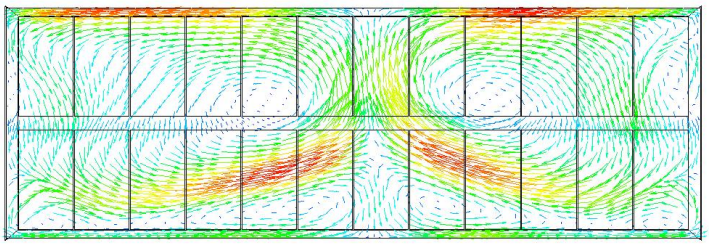 US	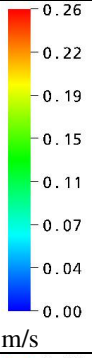
Side Riser End Bus Vmax = 0.235 m/s Vaverage= 0.076 m/s	DS 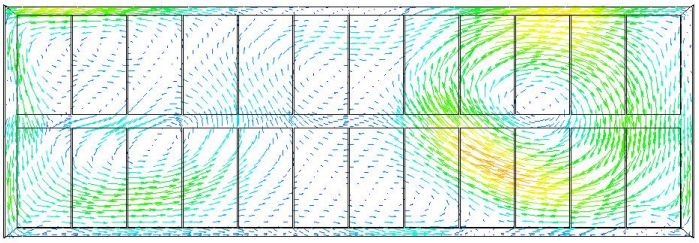 US	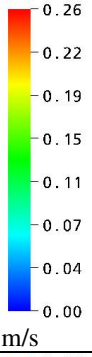
Side Riser Under Bus Vmax = 0.229 m/s Vaverage= 0.055 m/s	DS 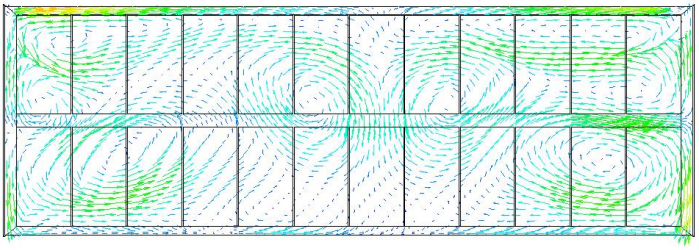 US	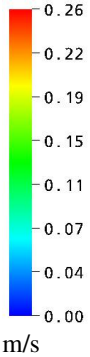

Metal flow statistics:

Model	Metal Velocities >2 cm/s & <10 cm/s	Metal Velocities <2 cm/s	Metal Velocities >10 cm/s
End Riser	46.6 %	3.9%	49.5%
Side Riser End Bus	63.6 %	7.8%	28.6%
Side Riser Under Bus	75.4 %	9.4%	15.3%

Metal Heave

The side riser options have a dramatic effect on flattening the metal contour, Figure A6. This has beneficial consequences for cell operations including current efficiency, metal purity and gross carbon consumption.

Figure A6. Metal Heave

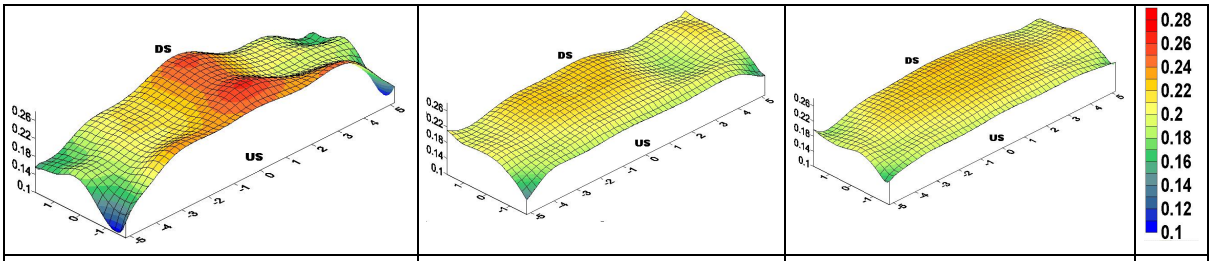

End Riser	Side Riser End Bus	Side Riser Under Bus	[m]
Zmax = 0.262 m Zmin = 0.103 m Δanode shadow = 0.159 m	Zmax = 0.225 m Zmin =0.137 m Δanode shadow = 0.088 m	Zmax = 0.226 m Zmin =0.155 m Δanode shadow = 0.071 m	

Stability

In order to compare the stability of the three designs, anode removal situations were simulated. The background flow for each technology (typical flow pattern) was first taken in account by calculating a transient flow analysis prior to the anode removal.

The typical oscillation periods (all anodes present) were calculated by performing a Power Spectral Density (PSD) analysis of the currents:

Model	Typical Oscilation Period [s]
End Riser	27.8
Side Riser End Bus	48.0
Side Riser Under Bus	26.7

After the removal of the anode in the highest B_Z location for each model (anode 13 for Side Riser Under Bus model; anode 12 for End Riser and Side Riser End Bus models), the pots

were monitored for 150 s each. Resulting transient currents in typical anodes (one in each pot headwall, one in pot center and one neighboring anode to the one removed) are shown in Figure A7. Note that the scale in the End Riser model is much wider than in the two Side Riser models.

Figure A8 shows the oscillating currents only (the average current for each anode is subtracted from the transient current). Comparing the two Side Riser options, it is seen that the Under Bus option produces a smaller oscillation and achieves a faster damping of the waves. Once again, the scale in the End Riser model is much wider than the two Side Riser models; as may be seen, its behavior regarding instability is much worse than either of the Side Riser models.

A PSD analysis for the remaining anodes after the removal operation is shown in Figure A9 and in the table below, confirming that the Side Riser Under Bus option has superior stability

Model	PSD Integral [A^2]
End Riser	$8.82*10^6$
Side Riser End Bus	$8.52*10^5$
Side Riser Under Bus	$4.89*10^5$

During the flow simulation following anode change, the energy transfer was also studied. It shows a very similar correlation with the spectral analysis. Figure A10 shows the (volume averaged) energy transfer for each time step, demonstrating the higher level of energy transfer after the anode removal for the less stable busbar options. The End Riser option presented a short circuit (metal touching the anodes) just after the anode removal, even at a higher ACD. This explains the very high value obtained by the integration of PSD and energy transfer volume for this busbar arrangement, an order of magnitude above the Side Riser options.

Comparison of busbar mass

Model	Risers (kg)	Cathode bus (kg)	Anode bus (kg)	Total (kg)	Mass/Design Current (kg/kA)
End Riser	4113	13344	7193	24650	102.7
Side Riser End Bus	4774	15451	2730	22955	95.6
Side Riser Under Bus	4774	17030	2730	24534	102.2

Figure A7. Transient Current in Selected Anodes for 150 Seconds After Anode Change

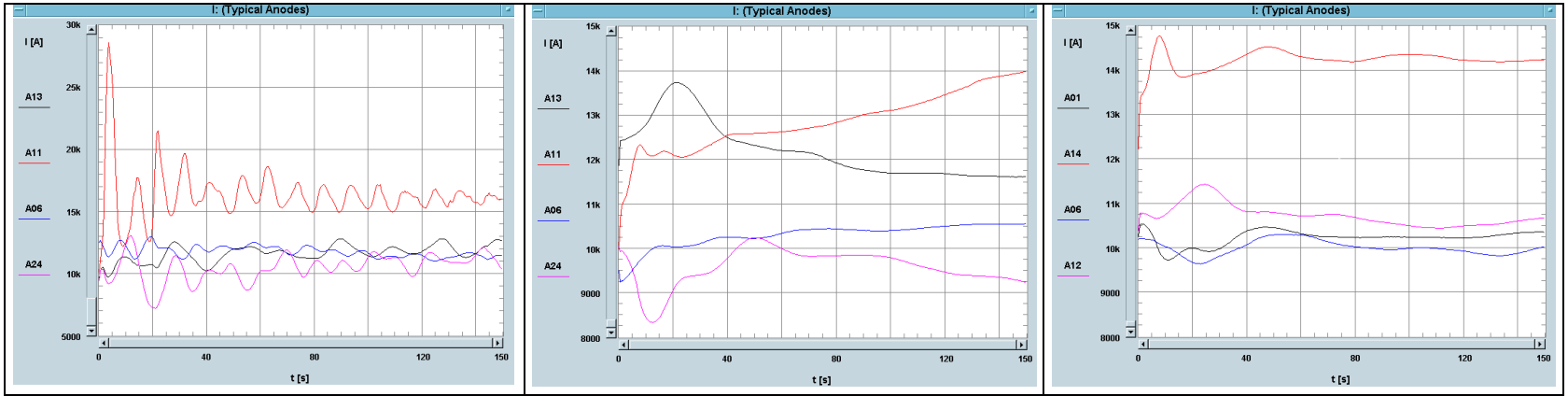

End Riser	Side Riser End Bus	Side Riser Under Bus

Figure A8. Oscillating Current in Selected Anodes for 150 Seconds After Anode Change

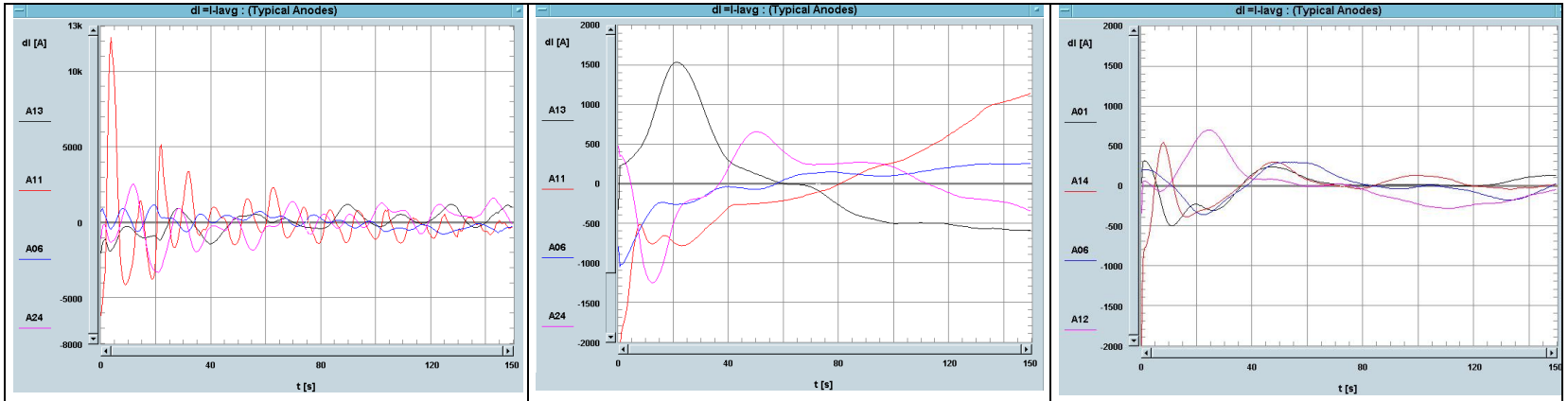

End Riser	Side Riser End Bus	Side Riser Under Bus

Figure A9 Power Spectral Density

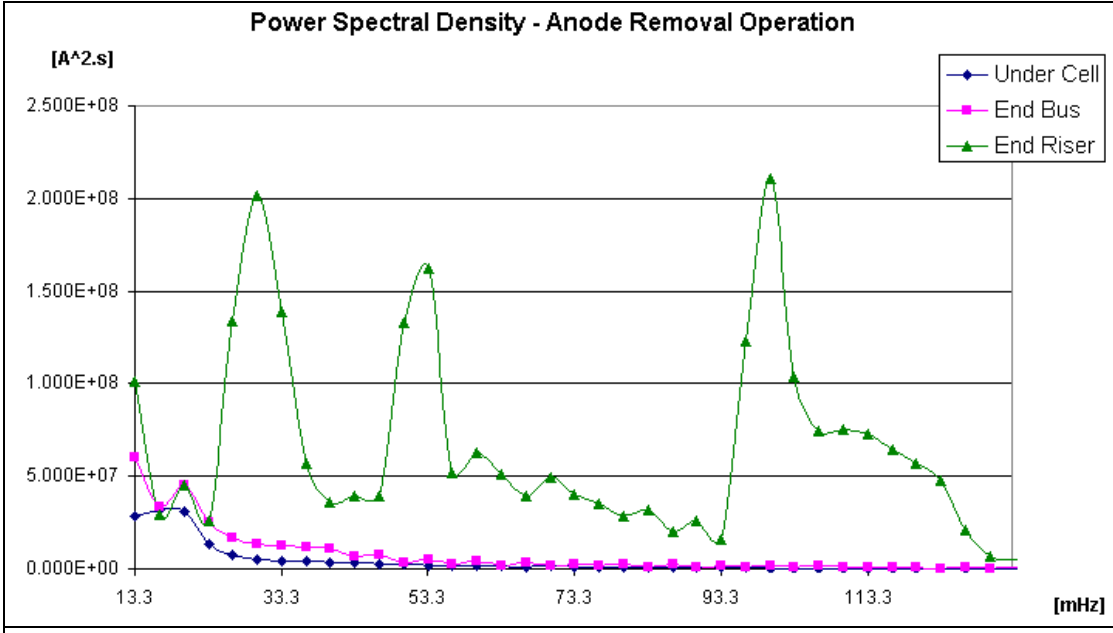

PSD Distribution for all models after the anode removal operation

Figure A10. Energy Transfer

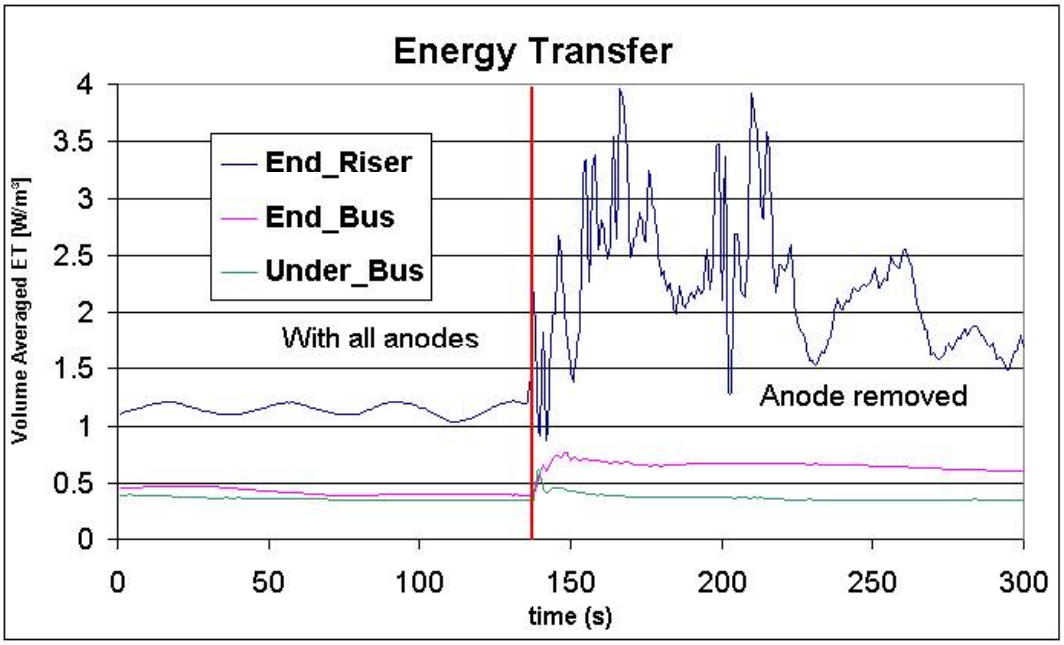

Energy Transfer Volume Averaged before and after the anode removal

References

[1] R. Huglen, Magnetic Compensation of Alumina Reduction Cells, *11th International Course on Process Metallurgy of Aluminium*, Trondheim, June 1992.

[2] M. Segatz & C. Droste, Analysis of Magnetohydrodynamic Instabilities in Aluminum Reduction Cells, *Light Metals* 1994

[3] V Potocnik, Principles of MHD Design of Aluminium Electrolysis Cells, *Magnetohydrodynamics in Process Metallurgy*, *The Minerals, Metals & Materials Society*, 1991

[4] A. F. LaCamera, Magnetohydrodynamics in the Hall-Heroult Process, an Overview, *Magnetohydrodynamics in Process Metallurgy The Minerals, Metals & Materials Society*, 1991

[5] M. Dupuis and I. Tabsh, Thermo-Electro-Magnetic Modeling of a Hall-Héroult Cell, *Proceeding of the ANSYS® Magnetic Symposium*, Sept 1994

[6] V. Potocnik, Modelling of Metal-Bath Interface Waves in Hall-Héroult Cells using ESTER/PHOENICS, *Light Metals* 1998

[7] C.W.Hirt, Volume of Fluid (VOF) Method for Free Boundaries, *J. Computational Physics* 1981

[8] A.D. Sneyd, Interfacial Instabilities in Aluminium Reduction Cells, *J. Fluid Mechanics, vol 236* 1992

[9] O. Zikanov, Shallow Water Model of Flows in Hall-Héroult Cells, *Light Metals* 2004

[10] V Potocnik, Principles of MHD Design of Aluminium Electrolysis Cells, *Magnetohydrodynamics in Process Metallurgy*, *The Minerals, Metals & Materials Society*, 1991

[11] C.H. Droste, Magnetohydrodynamic Stability Analysis in Reduction Cells, *Light Metals* 1998.

[12] Keinborg M et al, US Patent 4,592,821. June 3, 1986.

[13] V Potocnik & J.W. Evans, Evolution of Busbar Design in Hall-Heroult Cells and its Impact on the Process, CIM Conference, August 1986

[14] G.P. Brookes, Research and Development in a Project Environment, IE Aust Conference Gladstone, Australia, Sept 2002

[15] Austin Engineering Pty Ltd , 173 Cobalt Street, Carole Park, Brisbane, Queensland, Australia. 4300

[16] Meanderlyn Pty Ltd, 19 Foundation Road, Buderim, Queensland, Australia 4556

[17] H van de Nieuwelaar & M Ashriel, CADWELD Exothermic Welding, *Sixth Australasian Aluminium Smelter Technology Conference*, Queenstown New Zealand, November 1998.

[18] H. Luechinger, Not all busbars are equal, *Aluminium 80*, Jan 2004.

[19] J Purdie et al, Improving the Stability of the A817 Pot at Portland Aluminium, *Seventh Australasian Aluminium Smelter Technology Conference,* Melbourne Australia, November 2001

[20] G E da Mota & G J de Andrade, Magnetic Compensation Project at Albras Smelter, *Light Metals* 2001.

[21] D Vogelsang, Application of Integrated Simulation Tools for Retrofitting Aluminium Smelters, *Fourth Australasian Aluminium Smelter Technology Conference,* Sydney Australia, October 1992

[22] T Johansen et al, Productivity Increase at Soral Smelter, *Light Metals* 1999.